Food Research International 221 (2025) 117165

Contents lists available at ScienceDirect

Food Research International

journal homepage: www.elsevier.com/locate/foodres

The stressosome and SigB influence the baseline thermal resistance but not dynamic adaptation of *Listeria monocytogenes*: insights from kinetic modelling

Silvia Guillén [a,b], Pablo S. Fernández [a], Conor O'Byrne [c], Alberto Garre [a,*]

[a] Departamento de Ingeniería de Alimentos y del Equipamiento Agrícola, Instituto de Biotecnología Vegetal, Universidad Politécnica de Cartagena (ETSIA), Paseo Alfonso XIII, 48, 30203 Cartagena, Spain
[b] Departamento de Producción Animal y Ciencia de los Alimentos, Instituto Agroalimentario de Aragón - IA2 - (Universidad de Zaragoza-CITA), Zaragoza, Spain
[c] Bacterial Stress Response Group, Microbiology, School of Biological and Chemical Sciences, University of Galway, Ireland

ARTICLE INFO

Keywords:
Predictive microbiology
Geeraerd model
Stress acclimation
Stress response
Pasteurization
SigB
Stressosome

ABSTRACT

This study takes a first step towards incorporating a more mechanistic basis into current microbial inactivation models. We focus on the role of SigB and the stressosome in the heat resistance of *Listeria monocytogenes* using a reference strain (EGD-e), as well as five mutant strains where SigB and/or the stressosome were mutated. Data was analysed using the Geeraerd model to quantify the link between SigB/stressosome and thermal resistance. The Δ*sigB* strain had lower thermal resistance ($\log_{10}D_{58}$ = 0.21 $\log_{10}$ min) than EGD-e (0.27 $\log_{10}$ min). Mutations known to negatively affect the stressosome function also reduced the *D*-value (0.18 $\log_{10}$ min for RsbS S56A). Survivor curves had also a shoulder, which was also affected by SigB/stressosome. Exponential phase cells of the RsbR1-only strain had the shortest shoulder, while the wild type strain had the longest, which suggests that RsbR1 paralogues play a role in thermal stress response. Every strain was able to develop stress acclimation during dynamic heat treatments at low heating rates (2 °C/min) suggesting that factors other than SigB are important for thermal adaptation. Its impact was comparable to the jump from exponential to stationary phase cells, underlining the relevance of stress acclimation. This emphasizes the need for predictive models to go beyond a "baseline" resistance, accounting for the ability of cells to change their resistance as a response to environmental signals. This study marks a first step towards that goal, by defining possible ranges of variation for the *D*-value and shoulder length of *L. monocytogenes*.

1. Introduction

Thermal treatments are a fundamental part of food safety assurance, as high temperatures can inactivate most microbiological hazards in foods (Peng et al., 2017). However, high temperatures also induce other biochemical reactions in foodstuff, such as degradation of nutritional compounds, browning or texture changes, leading to a loss in nutritional and/or sensorial quality (Verbeyst, Bogaerts, Van der Plancken, Hendrickx, & Van Loey, 2013; Wang, Law, Mujumdar, & Xiao, 2017). Therefore, thermal treatments must be optimized to cause the required level of microbial inactivation with a minimum impact on product quality.

The optimization of heat treatments requires mathematical models able to predict the reduction in the microbial population for a given temperature profile. Microbial inactivation by heat is a highly complex process, which combines complex microbiological and thermodynamical principles (Smelt & Brul, 2014). As a result, current models from predictive microbiology apply strong simplifications at the population level, with state-of-the-art microbial inactivation models being based on empirical equations fitted to experimental data (Georgalis, Fernandez, & Garre, 2023).

Therefore, current models are constrained by the simplifications needed to construct them from limited datasets. A key aspect for this is that a large body of microbial inactivation models was built using reference strains. This design choice towards standardization might have under-represented bacterial strains with extreme phenotypes (Ma, Chen, Zwietering, Abee, & Den Besten, 2024). This is a critical point for risk assessment, as it has been hypothesized that foodborne outbreaks

* Corresponding author.
E-mail address: alberto.garre@upct.es (A. Garre).

https://doi.org/10.1016/j.foodres.2025.117165
Received 19 June 2025; Received in revised form 28 July 2025; Accepted 28 July 2025
Available online 5 August 2025

could be linked to bacterial strains with extreme phenotypes (den Besten, Aryani, Metselaar, & Zwietering, 2017; Zwietering, Garre, & den Besten, 2021). Furthermore, most models were built from microbial cultures grown under optimal growth conditions. Although this approach serves to quantify the "baseline" microbial resistance to heat, bacterial cells are dynamic entities that can adapt their physiology to the environmental conditions, as evidenced by several studies showing that cells pre-exposed to stressful conditions (either high temperature or other stresses) may increase their resistance to subsequent heat treatments through the development of (cross-) acclimation (Garre, González-Tejedor, Aznar, Fernández, & Egea, 2019; Heinrich et al., 2016; Valdramidis, Van Impe, & Geeraerd, 2006).

The bias introduced by the reduced pool of bacterial strains and physiological conditions is hard to quantify due to the lack of mechanistic parameters in current models. Hence, incorporating insight on the response to stress at the molecular level seems a promising avenue for improvement (Liu et al., 2025). In this context, *L. monocytogenes* serves as an excellent model organism for studying stress adaptation, given its genetic diversity and its ability to survive in diverse environmental conditions (Quereda et al., 2021). One of the major stress response mechanisms in *L. monocytogenes* that helps it survive under thermal, acidic, osmotic, and other stress conditions is the general stress response, which is under the control of the alternative sigma factor sigma B (SigB) (Liu, Orsi, Boor, Wiedmann, & Guariglia-Oropeza, 2017). SigB is responsible for the transcription of around 300 genes involved in the stress response and virulence (Guerreiro, Arcari, & O'Byrne, 2020; Oliver et al., 2009). Its activity is regulated by a complex signal transduction pathway, which is ultimately controlled by a multi-protein sensory hub known as the stressosome (Marles-Wright et al., 2008; NicAogáin & O'Byrne, 2016). The stressosome is a stress sensory complex composed of multiple copies of the RsbR protein and its homologs, as well as RsbS and RsbT. Upon encountering stress signals, the stressosome triggers a signal transduction cascade that ultimately leads to the release of SigB from the anti-sigma factor RsbW, thereby making it available to participate in transcription (NicAogáin & O'Byrne, 2016). Recent studies have focused on signal transduction mechanisms that activate the general stress response in *L. monocytogenes* in response to acidic and osmotic environments (Dessaux, Guerreiro, Pucciarelli, O'Byrne, & García-del Portillo, 2020; Guerreiro et al., 2022). Acid stress signals are integrated into the general SigB-dependent stress response pathway via the stressosome (Guerreiro et al., 2022). However, studies on heat stress response mechanisms in *L. monocytogenes* are limited, with few studies exploring the molecular pathways involved in its adaptation to high and sub-lethal temperatures (Ferreira, O'Byrne, & Boor, 2001; Somolinos, Espina, Pagán, & Garcia, 2010; van der Veen et al., 2007).

Based on that, the goal of this study is to advance our understanding of how those molecular mechanisms are linked to population level microbial inactivation kinetics for *L. monocytogenes*. We define a model built from exponential phase cells of *L. monocytogenes* EGD-e (type strain for *L. monocytogenes*) exposed to isothermal treatments as "baseline" microbial resistance. Then, we analyze how the stressosome and SigB are linked to changes in the thermal resistance of the population using a collection of *L. monocytogenes* mutants, including one with a deletion in the *sigB* gene, another where the *RsbR1* paralogs were deleted, a mutant with inactivated kinase activity of RsbT, and two mutants in which the putative phosphorylation sites in the stressosome core proteins RsbS and RsbR1 were substituted with alanine. The variability in the response is characterized further by modifying the status of the cells and treatment conditions (exponential vs stationary phase cells; isothermal vs dynamic treatments). The data are described using nonlinear inactivation models to enable a quantification of the changes in the initial (shoulder length) and overall (inactivation rate) thermal resistance of the population.

2. Materials and methods

2.1. Bacterial strain and culture conditions

L. monocytogenes EGD-e (serovar 1/2a, clonal complex 9, sequence type 35) and its mutants are indicated in Table 1. Strains were maintained frozen at −80 °C in cryovials with 0.7 % DMSO for long-term preservation. Strains were grown in a 100 mL flask containing 30 mL of Brain Heart Infusion (BHI) broth (Scharlau Chemie SA, Barcelona, Spain) at 37 °C with constant shaking at 150 rpm. Cells were grown for 24 h until stationary phase was reached (stationary phase cells) or further diluted in fresh BHI to an initial $OD_{600} = 0.05 \pm 0.01$ and further allowed to grow until mid-log phase ($OD_{600} = 0.4 \pm 0{,}02$) (exponential phase cells).

2.2. Thermal treatments and enumeration of survivors

Heat treatments were carried out in a Mastia thermoresistometer (Conesa, Andreu, Fernández, Esnoz, & Palop, 2009). Briefly, this instrument consists of a 400 mL vessel equipped with an electrical heater and cooling system, a stirring device to ensure inoculum distribution and temperature homogeneity, and ports for the injection of microbial suspension and for the extraction of samples. For isothermal treatments, once the temperature inside the vessel stabilized (±0.1 °C) at the treatment temperature (55–62 °C), 0.2 mL of cell suspension (in stationary or exponential growth phase) were injected into the main chamber containing Brain Heart Infusion (BHI) broth (Scharlau). For treatments under dynamics conditions, experiments were conducted using two biphasic temperature profiles in which the heating medium was heated from the initial temperature (30 °C) to the target temperature (58 °C) at four different heating rates (2, 5, 10 and 14 °C/min). In these experiments, the treatment medium was inoculated with 0.2 mL of exponential phase cell suspension once the thermoresistometer had reached the initial temperature. After inoculation under both conditions, samples were collected at different heating times. Samples were adequately diluted in Buffered Peptone Water (BPW; Oxoid; Basingstoke, UK) and plated in the recovery medium, BHI agar (Scharlau). Plates were then incubated for 48 h at 37 °C, after which the colony-forming units (CFU) per plate were counted. For each condition, thermal experiments were performed for three independent biological replicates.

2.3. Analysis of data obtained under isothermal conditions

The survivor curves obtained under isothermal conditions were nonlinear with clear shoulders. This was confirmed by fitting log-linear and non-linear models (also Weibullian models) to the data using *AIC* for model selection. Therefore, they were described using the algebraic solution of the Geeraerd model for curves without a tail (Geeraerd, Herremans, & Van Impe, 2000). The model is shown in Eq. (1), where N is the microbial concentration and t is the treatment time. The microbial

Table 1
Strains collection of *L. monocytogenes* used in this study.

Strains	Reference
Listeria monocytogenes EGD-e (Wild Type (WT))	Conor P. O'Byrne
L. monocytogenes EGD-e Δ*sigB*	Guerreiro et al. (2020)
L. monocytogenes EGD-e (ΔrsbL ΔrsbR2 ΔrsbR3 ΔrsbR4 (RsbR1-only))	Guerreiro et al. (2022)
L. monocytogenes EGD-e (rsbS S56A)	Guerreiro et al. (2022)
L. monocytogenes EGD-e (rsbT N49A)	Dessaux et al. (2020)
L. monocytogenes EGD-e (rsbR1 T241A)	Guerreiro et al. (2022)

kinetics are described by the inactivation rate, k, and the shoulder length, S_l.

$$N = N_0 e^{-kt} \frac{e^{kS_l}}{1 + (e^{kS_l} - 1)e^{-kt}} \quad (1)$$

The secondary models were defined based on the recommendations by Garre, Valdramidis, and Guillén (2025). Accordingly, if we use a log-linear secondary model for k (Eq. 2), the only secondary model for S_l compatible with the dynamic assumptions of the Geeraerd model would also be log-linear (Eq. 3).

$$\ln k = a + b \cdot T \quad (2)$$

$$S_l = A e^{-b \cdot T} \quad (3)$$

The secondary model for k is defined by the intercept (a) and slope (b) terms, as broadly accepted in predictive microbiology. However, according to Garre, Valdramidis, and Guillén (2025), the secondary model for S_l is linked to the other secondary model, as b appears in both equations and the coefficient A is defined as $A = e^{-a}\ln(Q_0 + 1)$. Hence, it only adds an additional unknown parameter (Q_0).

To facilitate the biological interpretation of the model fits, the model was reparameterized based on the D-value (time for one log-reduction at constant temperature) and the z-value (temperature increase required for a 10-fold reduction of the D-value). Accordingly, instead of the regression parameters a and b, we used the identities in Eqs. (4–6). This introduces a reference temperature (T_{ref}), so the D-value is defined at the reference temperature (D_{ref}). The reference temperature has no biological meaning but improves parameter identifiability (Peñalver-Soto, Garre, Esnoz, Fernández, & Egea, 2019). T_{ref} was fixed at 58 °C to facilitate the interpretation of the dynamic results, as this is the maximum temperature in those experiments.

$$z = \frac{\ln 10}{b} \quad (4)$$

$$\ln k_{ref} = a - b \cdot T_{ref} \quad (5)$$

$$D_{ref} = \frac{\ln 10}{k_{ref}} \quad (6)$$

The microbial response is thus described by three unknown parameters (D_{ref}, z and Q_0) plus the initial microbial concentration N_0. These parameters were estimated in one step by nonlinear regression (i.e., estimating the values of the four parameters by least squares from the observed log-microbial concentrations at the different treatment temperatures). This was implemented in R version 4.2.3 (R Core Team, 2022) using version 1.3.6.2 of the FME package (Soetaert & Petzoldt, 2010), which implements the Newton-Raphson algorithm (Bates & Watts, 2007). To facilitate convergence, the values of Q_0, N_0 and D_{ref} were $\log_{10}$-transformed for model fitting. The fit was assessed using the Root Mean Squared Error: $RMSE = \sqrt{\frac{1}{n}\sum \left(\log_{10} N_{obs} - \log_{10} N_{pred}\right)^2}$.

The models were fitted independently to the data obtained from each strain (6 strains) and for each physiological state (exponential or stationary phase cells), resulting in 12 independent models. The computer code is available in the GitHub page of one of the coauthors (https://github.com/albgarre/sigB_Listeria).

2.4. Model predictions under dynamic temperature conditions

The data obtained under dynamic temperature conditions was analysed using the dynamic version of the Geeraerd model (i.e., based on differential equations). This model is shown in Eq. (7), where α and β introduce, respectively, the shoulder and tail effects. Considering neither the isothermal nor the dynamic data showed tails, the coefficient β was set to one.

$$\frac{dN}{dt} = -\alpha \cdot k \cdot \beta \cdot N \quad (7)$$

The coefficient $\alpha = \frac{1}{1+Q}$ introduces the shoulder under the assumption of a theoretical substance (Q) that has a protective effect. This model assumes that Q follows first order inactivation kinetics with rate k (Eq. 8).

$$\frac{dQ}{dt} = -k \cdot Q \quad (8)$$

Hence, the duration of the lag phase is defined by the initial value of Q (Q_0), which is related to the lag phase duration under isothermal conditions by the identity $S_l = \frac{\ln(Q_0+1)}{k}$ (Valdramidis, Van Impe, & Geeraerd, 2006).

Therefore, the predictions of this model are characterized by Q_0, as well as the secondary model for k (note that the dynamic model does not require a secondary model for S_l, as this is only defined for isothermal experiments). For compatibility with the model used for isothermal conditions, a log-linear model for k was also used (Eq. 2).

Comparing the predictions of models obtained under isothermal conditions against data obtained under dynamic temperature conditions enables assessing the relevance of stress acclimation and similar effects (Garre et al., 2019; Valdramidis, Geeraerd, Bernaerts, & Van Impe, 2006). These were calculated by solving the differential equation (Eqs. 4 and 5) for the parameter values estimated from the isothermal data as described in section 2.3. The numerical calculations were performed using version 0.0.99 of the bioinactivation2 package for R (Garre, Georgalis, Lindqvist, & Fernandez, 2025), currently available in GitHub (https://github.com/albgarre/bioinactivation2).

The predictions of the models obtained under isothermal conditions against the observations obtained under dynamic conditions were evaluated using the *RMSE* and the Mean Error: $ME = \frac{1}{n}\sum \left(\log N_{obs} - \log N_{pred}\right)$.

2.5. Model fitting to data obtained under dynamic temperature conditions

The comparison based on the *ME* showed significant deviations between the model predictions obtained from data under isothermal conditions and the observations under dynamic conditions. Therefore, in order to better quantify the effect of the heating rate on thermal inactivation, the Geeraerd model was fitted directly to the dynamic data.

Models were fitted using the *bioinactivation2* package, that is based on the approach described for *bioinactivation* (Garre, Fernández, Lindqvist, & Egea, 2017). Briefly, model fitting can be defined as an optimization problem, consisting in finding the parameter values that minimize the *RMSE* of the predictions of the Geeraerd model against the microbial observations under dynamic conditions. The problem is solved by the Levenberg-Marquardt algorithm (Moré, 1978), using the interface implemented in *FME* (Soetaert & Petzoldt, 2010).

The Geeraerd model without tail (defined from D_{ref}, N_0, Q_0, z) was fitted independently for each strain and for each heating rate. To facilitate the evaluation of the increased resistance from isothermal to dynamic treatments, the fit was done by fixing the z-value to the one estimated under isothermal conditions for each strain.

3. Results

3.1. Thermal inactivation of L. monocytogenes under isothermal conditions

In this study, the thermal resistance of five *Listeria monocytogenes* EGD-e mutants was evaluated and compared against the wild type strain. The cells were analysed in two growth phases, exponential and stationary, and tested at three different temperatures per phase, ranging from 55 to 62 °C. The Geeraerd model with linked secondary models for

Table 2
Parameters of the Geeraerd model estimated from the data for exponential phase cells of *Listeria monocytogenes* under isothermal treatments, using a one-step method considering coupling between secondary models.

Strain	$\log_{10} Q_0$ (·)	$\log_{10} D_{58}$ ($\log_{10}$ min)	z (°C)	$\log_{10} N_0$ ($\log_{10}$ CFU/mL)	RMSE ($\log_{10}$ CFU/mL)
EGD-e (WT)	0.93 ± 0.17	0.27 ± 0.02	6.0 ± 0.1	5.22 ± 0.07	0.28
Δ*sigB*	0.77 ± 0.24	0.21 ± 0.02	7.2 ± 0.2	5.22 ± 0.10	0.45
RsbR1-only	−0.19 ± 0.53	0.30 ± 0.02	6.0 ± 0.1	5.35 ± 0.12	0.42
rsbS S56A	0.51 ± 0.29	0.18 ± 0.02	7.5 ± 0.2	5.13 ± 0.12	0.40
rsbT N49A	0.00 ± 0.32	0.26 ± 0.01	6.4 ± 0.1	5.19 ± 0.10	0.33
rsbR1 T241A	0.19 ± 0.29	0.43 ± 0.02	5.8 ± 0.1	5.29 ± 0.09	0.34

k and S_l was successful at describing the data obtained under isothermal conditions. This is illustrated in supp. Figs. 1 and 2, which depict the fitted curves against the microbial concentrations observed and shows that the observations clearly had a shoulder for all six strains tested. This implies that the temperature levels, despite being high enough to cause microbial inactivation in the long term, were ineffective at causing cell death from the onset of the treatment. Please note that the Mastia thermoresistometer includes continuous stirring and temperature control during the process (Conesa et al., 2009), so this initial shoulder is not an artefact of the inoculation.

The fact that all strains, including the Δ*sigB* mutant, showed this shoulder suggests that SigB function does not play a main role in this early-stage heat protection. Also, as illustrated in Tables 2 and 3, the *RMSE* of the model fits was reasonable for a one-step fitting algorithm (*RMSE* = 0.8 $\log_{10}$ CFU/mL in the worst case), further supporting the conclusion that the model was able to describe the general trend in the data.

In general, the data evidences that SigB contributes to resistance against thermal inactivation. Additionally, mutations that are known to negatively affect stressosome function (RsbS S56A and RsbT N49A) show increased sensitivity compared to the WT strain EGD-e. In particular, Table 2 reports the parameter values of the Geeraerd model estimated for exponential phase cells of each strain. The z-values ranged between 5.8 and 7.5 °C, values that are typical for vegetative cells (van Asselt & Zwietering, 2006). On the other hand, parameter D_{58} defines the thermal resistance at the reference temperature (58 °C). Hence, provided the z-value is comparable, higher values of D_{58} indicate a generally higher resistance. Accordingly, exponential phase cells of rsbR1 T241A would have the highest thermal resistance at the reference temperature ($\log_{10} D_{58}$ = 0.43 log min), followed by RsbR1-only (0.30 $\log_{10}$ min), EGD-e (0.27 $\log_{10}$ min), rsbT N49A (0.26 $\log_{10}$ min), Δ*sigB* (0.21 $\log_{10}$ min) and rsbS S56A (0.18 $\log_{10}$ min).

Stationary phase cells of every *L. monocytogenes* strain tested had a higher thermal resistance than exponential phase ones. This is evidenced by parameter logD_{58} having significantly higher values for every strain (0.86 vs 0.27 $\log_{10}$ min for the wild type, 0.62 vs 0.21 $\log_{10}$ min for the Δ*sigB* strain and 0.80 vs 0.30 $\log_{10}$ min for the RsbR1-only strain). Furthermore, stationary phase cells were less sensitive to temperature changes, as demonstrated by their generally lower z-values (4.7 vs 6.0 °C for the wild type, 4.3 vs 7.2 °C for the Δ*sigB* strain and 5.0 vs 6.0 °C for the RsbR1-only strain) (Table 3).

The results are aligned with previous studies on the thermal inactivation of *L. monocytogenes*. Based on a systematic literature review of 940 *D*-values reported for stationary-phase cells, van Asselt and Zwietering (2006) estimated a z-value of 7.0 °C and a *D*-value of 0.65 min at 58 °C. The z-value estimated by meta-regression is higher than the one obtained here, most likely due to the presence of experimental bias in that dataset (Garre, Zwietering, & den Besten, 2023). By looking at individual studies, our results are comparable to those reported by Szlachta, Keller, Shazer, and Chirtel (2010) ($\log_{10} D_{58} = 0.49 \log_{10}$min; $z = 5.7^{\circ}C$) or by Mazzotta and Gombas (2001) ($\log_{10} D_{58} = 0.46 \log_{10}$min; $z = 4.9^{\circ}C$). In fact, the mean of the log *D*-values reported in *D database* for *L. monocytogenes* for stationary phase cells in laboratory media is 0.42 log min (https://foodmicrowur.shinyapps.io/Ddatabase/), confirming the robustness of our experimental approach.

The secondary models for the *D*-value fitted for each strain for both stationary phase and exponential phase cells are depicted in Fig. 1A and B, respectively. In general, the Δ*sigB* strain showed the lowest *D*-values in both growth-phases and across the entire temperature range assayed. This is likely due to differences in gene expression between the Δ*sigB* mutant and WT strain that were present in the culture prior to thermal challenge (Guerreiro et al., 2020). It is possible that SigB could also be playing a role in the initial thermal resistance, as evidenced by the shorter shoulder length in the Δ*sigB* mutant.

Stationary phase cells had a higher thermal resistance than exponential phase cells, with higher *D*-values over the complete temperature range tested. The RsbR1-only mutant was similar in terms of resistance to the WT strain for both exponential and stationary phase cells. Among exponential phase cells, rsbR1 T241A strain showed the highest resistance, with higher *D*-values over the whole temperature range tested. Regarding the other strains, it is interesting that the differences between them are more relevant at 55 °C than at 60 °C, with the secondary models seeming to converge towards the highest temperature tested. This suggests that differences between strains for exponential phase cells are more apparent during treatments at lower temperatures, where longer exposure times are required for inactivation and presumably more time is available for any thermal acclimation to take place.

For the interpretation of the results, it is important to underline that the mode of inactivation represented by the shoulder is different from the one quantified by the *D*-value. Whereas the *D*-value describes the rate of inactivation during the lethal phase of the treatment, S_l defines the duration of the first phase, where the damage produced by the treatment is ineffective at causing cell death (Ruiz, Alonso, Salvador, Condón, & Condón-Abanto, 2021). The shoulder length often varies independently of the *D*-value, being affected by the physiological state of the cells, the type of heating medium or environmental conditions such as pH or temperature (Huang, 2009; Miller et al., 2009; Wang et al., 2024; Wang, Devlieghere, Geeraerd, & Uyttendaele, 2017) Therefore, it

Table 3
Parameters of the Geeraerd model estimated from the data for stationary phase cells of *Listeria monocytogenes* under isothermal treatments, using a one-step method considering coupling between secondary models.

Strain	$\log_{10} Q_0$ (·)	$\log_{10} D_{58}$ ($\log_{10}$ min)	z (°C)	$\log_{10} N_0$ ($\log_{10}$ CFU/mL)	RMSE ($\log_{10}$ CFU/mL)
EGD-e (WT)	0.99 ± 0.44	0.86 ± 0.04	4.7 ± 0.2	6.04 ± 0.18	0.82
Δ*sigB*	−0.09 ± 0.61	0.62 ± 0.03	4.3 ± 0.1	6.11 ± 0.16	0.53
RsbR1-only	1.67 ± 0.27	0.80 ± 0.03	5.0 ± 0.1	5.96 ± 0.09	0.50

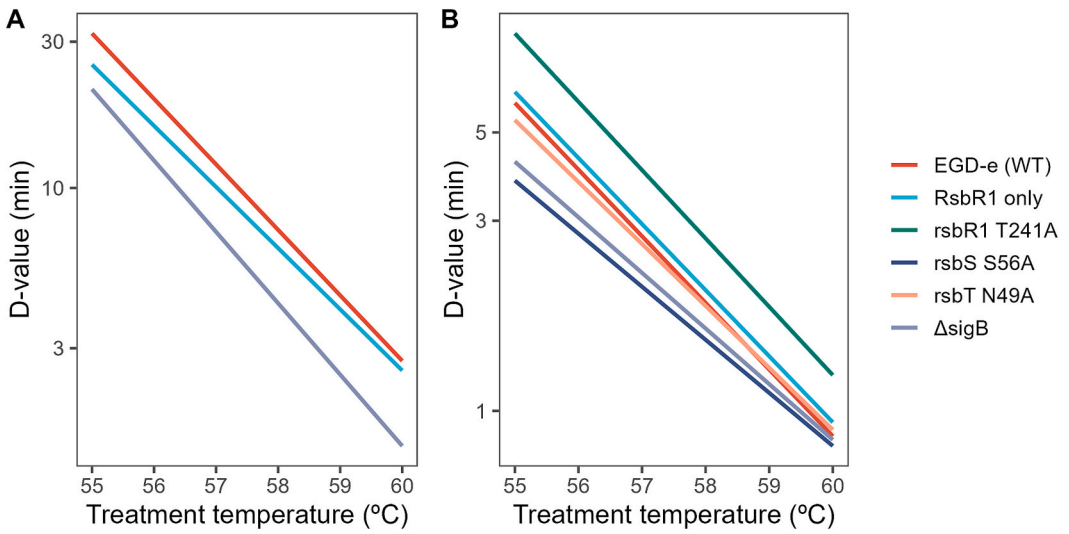

Fig. 1. Secondary model for the effect of temperature on the inactivation rate (Eq. 2) estimated from the data on the inactivation of *L. monocytogenes* at isothermal conditions for cells in stationary (A) or exponential (B) phase.

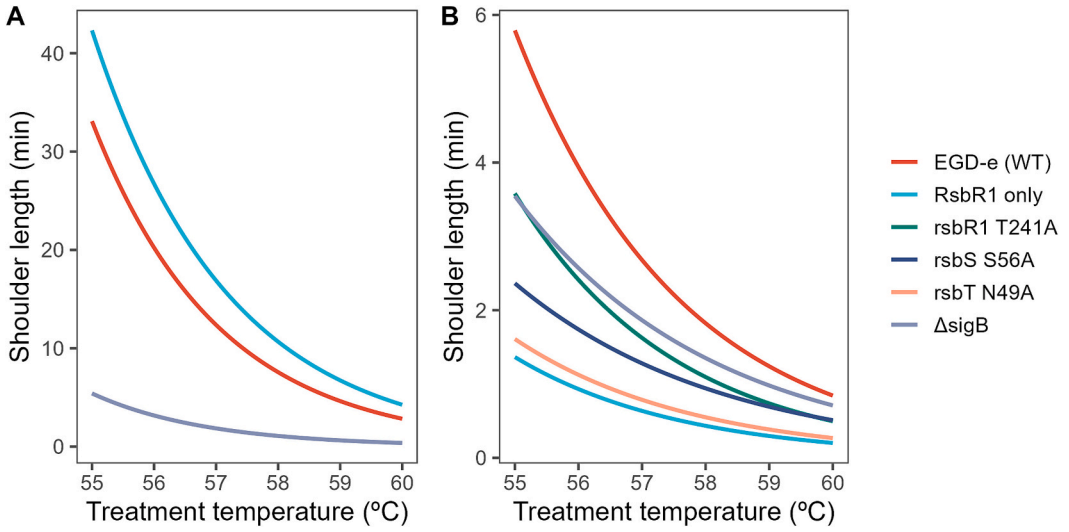

Fig. 2. Secondary model for the effect of temperature on the shoulder length (Eq. 3) estimated from the data on the inactivation of *L. monocytogenes* at isothermal conditions for cells in stationary (A) or exponential (B) phase.

merits an independent analysis.

In the Geeraerd model, the duration of this phase depends on a combination of the "physiological state" (quantified by Q_0, with higher values meaning "more resistant") and the *D*-value at the treatment temperature (defined by D_{ref} and z) (Geeraerd et al., 2000). To facilitate interpretation, Fig. 2 depicts the secondary models fitted to each strain using cells in the stationary phase (Fig. 2 A) or the exponential phase (Fig. 2B). It is evident that stationary phase cells had generally longer shoulders, showing that populations in this stage have higher thermal resistance. The only exception is the Δ*sigB* mutant, which showed practically the same shoulder length for both stationary and exponential phase cells. This shows that the shoulder is likely due to the establishment of a robust general stress response during stationary phase, likely mediated by SigB. As a result, stationary phase cells of the Δ*sigB* strain have the lowest S_l by far, underlining its lower heat resistance (it also had the lowest *D*-value). On the other hand, exponential phase cells of the Δ*sigB* mutant had intermediate shoulder.

Although stationary phase cells of WT and the RsbR1-only strain exhibited similar shoulders across the range of temperatures tested, exponential phase cells showed large differences. The RsbR1-only strain had the shortest shoulder length among all strains tested, while the wild type strain had the longest. Similar to the secondary model for the *D*-value, at low temperature (55 °C) the differences in shoulder length between strains were more pronounced than at high temperatures (60 °C). However, they appear to converge into several groups: RsbR1-only and rsbT N49A, or rsbS S56A and rsbR1 T241A, unlike for the *D*-value where every strain seemed to converge to a single one.

Table 4
ME ($\log_{10}$ CFU/mL) of the predictions of the Geeraerd models fitted to isothermal data from exponential phase cells of *L. monocytogenes* against the concentrations observed during dynamic treatments of different heating rates.

	2 °C/min	5 °C/min	10 °C/min	14 °C/min
EGD-e (WT)	−4.2	−1.8	−0.5	−0.3
RsbR1-only	−4.3	−2.1	−0.9	−0.7
rsbR1 T241A	−2.7	−1.1	−0.2	−0.1
rsbS S56A	−6.1	−3.0	−1.4	−1.1
rsbT N49A	−4.9	−2.4	−1.1	−0.9
Δ*sigB*	−5.4	−2.5	−1.0	−0.8

Table 5
Parameters of the Geeraerd model estimated from data obtained for different dynamic temperature conditions.

Heating rate	Strain	$\log_{10} N_0$ ($\log_{10}$ CFU/mL)	$\log_{10} D_{58}$ ($\log_{10}$ min)	$\log_{10} Q_0$ (·)	RMSE ($\log_{10}$ CFU/mL)
2 °C/min	EGD-e (WT)	5.26 ± 0.08	0.58 ± 0.02	2.55 ± 0.33	0.37
	RsbR1-only	5.24 ± 0.05	0.62 ± 0.02	1.89 ± 0.18	0.21
	rsbR1 T241A	5.24 ± 0.04	0.52 ± 0.02	3.79 ± 0.26	0.19
	rsbS S56A	5.30 ± 0.07	0.59 ± 0.02	2.42 ± 0.27	0.30
	rsbT N49A	5.16 ± 0.04	0.52 ± 0.02	3.06 ± 0.24	0.21
	Δ*sigB*	5.20 ± 0.09	0.66 ± 0.03	2.11 ± 0.35	0.39
5 °C/min	EGD-e (WT)	5.03 ± 0.03	0.61 ± 0.02	1.46 ± 0.16	0.17
	RsbR1-only	5.31 ± 0.06	0.46 ± 0.03	1.48 ± 0.25	0.25
	rsbR1 T241A	5.07 ± 0.03	0.59 ± 0.02	1.86 ± 0.14	0.17
	rsbS S56A	5.17 ± 0.05	0.52 ± 0.01	1.36 ± 0.14	0.22
	rsbT N49A	5.13 ± 0.03	0.51 ± 0.01	1.32 ± 0.09	0.13
	Δ*sigB*	5.24 ± 0.09	0.55 ± 0.02	0.04 ± 0.36	0.37
10 °C/min	EGD-e (WT)	5.03 ± 0.07	0.44 ± 0.03	1.34 ± 0.27	0.33
	RsbR1-only	5.13 ± 0.05	0.4 ± 0.02	1.22 ± 0.16	0.23
	rsbR1 T241A	5.21 ± 0.05	0.49 ± 0.02	1.24 ± 0.18	0.21
	rsbS S56A	4.95 ± 0.11	0.38 ± 0.02	0.18 ± 0.33	0.30
	rsbT N49A	5.19 ± 0.08	0.26 ± 0.02	0.38 ± 0.22	0.22
	Δ*sigB*	5.26 ± 0.08	0.38 ± 0.02	0.41 ± 0.25	0.30
14 °C/min	EGD-e (WT)	5.08 ± 0.05	0.28 ± 0.02	1.91 ± 0.21	0.19
	RsbR1-only	5.04 ± 0.04	0.26 ± 0.02	2.25 ± 0.24	0.20
	rsbR1 T241A	5.09 ± 0.05	0.39 ± 0.04	2.02 ± 0.33	0.21
	rsbS S56A	4.98 ± 0.07	0.18 ± 0.02	2.02 ± 0.24	0.25
	rsbT N49A	5.19 ± 0.07	0.26 ± 0.02	1.31 ± 0.18	0.26
	Δ*sigB*	5.15 ± 0.09	0.34 ± 0.02	0.44 ± 0.26	0.28

3.2. Thermal inactivation of L. monocytogenes under dynamic conditions

The Geeraerd models built based on data gathered under isothermal conditions from cells on the exponential phase were used to predict the microbial response during treatments with varying temperatures. As illustrated in Supp. Figs. 3–6, there were clear deviations between the model predictions and the observations, with the microbial concentrations being consistently higher than the model predictions. Table 4 quantifies the magnitude of these deviation using the *ME*. For the highest heating rate tested (14 °C/min), the *ME* is relatively low (mean of 0.8 $\log_{10}$ CFU/mL), showing a good predictive power. However, this index grows for lower heating rates (mean *ME* of 5 $\log_{10}$ CFU/mL for 2 °C/min), demonstrating that the model predictions overpredict the microbial concentration for these conditions.

Similar effects have already been reported in the literature and have been attributed to a dynamic stress adaptation (Clemente-Carazo, Cebrián, Garre, & Palop, 2020; Garre et al., 2019; Garre, Egea, Iguaz, Palop, & Fernandez, 2018). Accordingly, as the temperature during the heating phase in our design grows linearly from 30 to 58 °C, the microbial population is exposed to sublethal temperatures during a large part of the treatment. Despite not causing noticeable inactivation, sublethal temperatures would still activate the stress-response mechanisms of the bacterial cells. As a result, if the heating is slow, the thermal resistance of the cells would be increased due to the activation of the stress-response mechanisms resulting in deviations with respect to the predictions of the isothermal model (where the heating is practically instantaneous). On the other hand, if the heating is fast, the microbial population cannot acclimate before being exposed to lethal temperatures, so there are practically no deviations with respect to model predictions based on isothermal data.

To quantify the increase in thermal resistance during dynamic treatments, the Geeraerd model was fitted directly to the data obtained under dynamic conditions. Supp. Figs. 3–6 show the adequate model fit, with Table 5 reporting the parameter estimates. Fig. 3 provides an overall view of the thermal resistance for the different conditions studied here, both for isothermal and dynamic treatments, based on the Geeraerd model. Fig. 3A depicts the *D*-value estimated at the reference temperature (58 °C; the maximum of the dynamic heating profile). Every strain tested was able to develop stress acclimation during dynamic heating profiles, showing higher *D*-values under dynamic conditions than isothermal ones (please note that dynamic experiments were performed with cells on the exponential growth phase). In line with previous research (Clemente-Carazo et al., 2020; Garre et al., 2019), the difference was dependent on the heating rate. While microbial populations exposed to the highest heating rate (14 °C) had the same *D*-value as exponential phase cells exposed to isothermal conditions, lower heating rates resulted in higher *D*-values, as predicted based on stress acclimation. The effect of stress acclimation was substantial, clearly overshadowing the effect of strain variability under isothermal conditions (within the pool of strains considered here).

Despite the strains showing high variability for isothermal treatments (Fig. 1), the highest *D*-value observed under dynamic conditions seemed to stabilize around 0.55 $\log_{10}$ min (3.5 min) for every strain. This is in agreement with previous results, showing that bacterial strains with higher "baseline" thermal resistance (under isothermal conditions) would have a lower ability to develop stress acclimation (Georgalis, Psaroulaki, Aznar, Fernández, & Garre, 2022).

Fig. 3A also illustrates the differences between stationary phase cells exposed to isothermal treatments and dynamic stress acclimation. For the WT strain and the RsbR1-only mutant, stationary phase cells had a higher thermal resistance than cells exposed to a dynamic treatment with a heating rate of 2 °C/min. However, cells of the Δ*sigB* mutant exposed to a heating rate of 2 °C/min had a similar *D*-value as stationary phase cells. This result emphasizes the relevance of the physiological state of the cells on the thermal resistance of the population, with the type of treatment having a larger effect than strain variability. It also emphasizes the relevance of the heating rate, as slow heating rates caused an increase in thermal resistance comparable to the jump from exponential to stationary phase cells, presumably due to the time needed to mount an effective transcriptional response.

As depicted in Fig. 3B, the heating rate had a rather significant effect on the apparent shoulder length at 58 °C. Note that these values are estimated from $\log Q_0$ and k_{ref}, so they should not be interpreted directly from the graphs shown in supp. Figs. 3–6 (where the apparent shoulder is due to the low temperature at the beginning of the treatment). This effect on the shoulder (through Q_0) had not been reported in previous acclimation studies, partly due to the lack of a clear link between isothermal and dynamic conditions. Using the model by Garre, Valdramidis, and Guillén (2025), we are able to establish this link, showing that stress acclimation might induce longer shoulders.

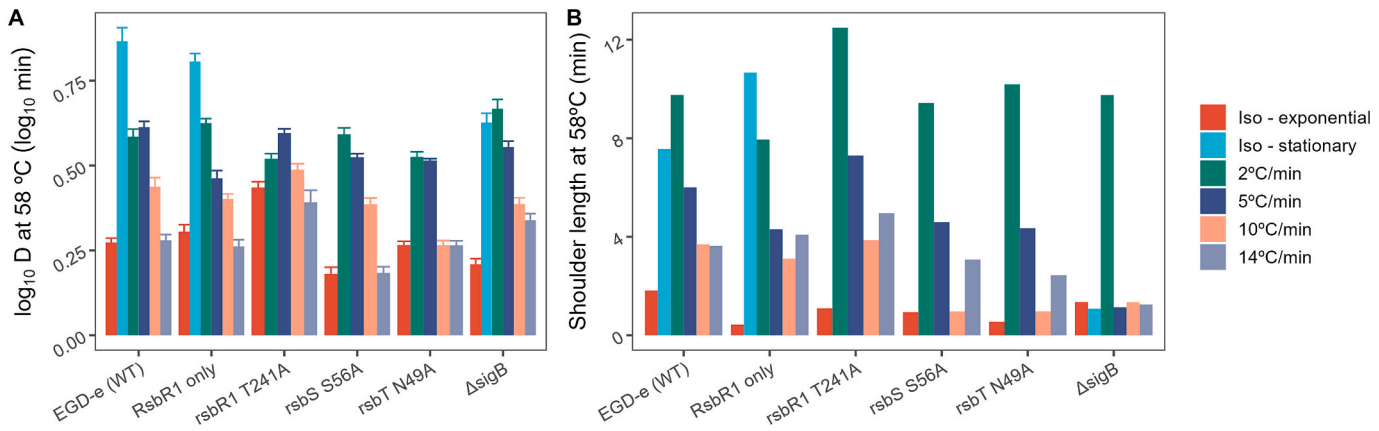

Fig. 3. Comparison between the *D*-value and S_l estimated by the models obtained under isothermal ("Iso") or dynamic heating conditions (with different heating rates) at a reference temperature of 58 °C for six different strains of *L. monocytogenes*. Isothermal experiments were done for cells in the exponential ("Iso – exponential") and stationary ("Iso – stationary") growth phases, while dynamics experiments were performed with cells in exponential growth phase. The height of the bar represents the estimated value, with error bars showing the standard errors. Note that the shoulder length does not show error bars because this parameter is not estimated directly (it is calculated from $\log Q_0$ and k_{ref}).

Qualitatively, the effect of the heating rate on the shoulder length was similar to the one it had on the *D*-value, with lower heating increasing the thermal resistance. However, from a quantitative standpoint, the effect was more noticeable. Even the highest heating resulted in an increase in shoulder length with respect to the one observed under isothermal conditions, with the only exception being the Δ*sigB* strain. The slowest heating caused roughly a 5-fold increase in the shoulder length of the bacterial population. This resulted for the WT and Δ*sigB* strains in longer shoulders than for stationary phase cells, although the RsbR1-only mutant the shoulder under stationary phase was still longer. This result underlines further the relevance of the heating rate on the thermal resistance of the population.

4. Discussion

4.1. SigB has a key role in the inactivation kinetics of L. monocytogenes

The alternative sigma factor SigB is the master regulator of stress resistance genes in Gram-positive genera, such as *Listeria* and *Bacillus*. SigB has been shown to play a crucial role in resistance or adaptation to various stress conditions, such as heat, acid, osmotic stress, light and pulsed electric fields, among others (Dessaux et al., 2020; Dorey, Lee, Rotter, & O'Byrne, 2019; Ferreira et al., 2001; Guerreiro et al., 2022; Somolinos et al., 2010). Despite this evidence, current kinetic models do not include information on the activation of the stressosome or SigB.

One key factor in SigB induction is the growth phase of the bacterial population. It has been demonstrated that *L. monocytogenes* cells have maximal SigB activity when cells enter the stationary phase (Nadal, Mañas, & Cebrián, 2024; Utratna, Cosgrave, Baustian, Ceredig, & O'Byrne, 2014). This is in line with our observations, as heat resistance of stationary phase cells in isothermal conditions was found to be SigB-dependent under the conditions evaluated. The deletion of *sigB* led to a consistent reduction in thermal resistance in every condition tested (exponential cells, stationary cells and dynamic treatments). This underlines that SigB is key for the survival of *L. monocytogenes*, in line with previous research (Hu et al., 2007; Ma et al., 2024; Somolinos et al., 2010). It is thus clear that SigB, at least partly, contributes to the difference in thermal tolerance between exponential and stationary phase. The precise signals that trigger the activation of SigB in stationary phase are unknown but could include changes in pH, cell density, organic acid levels or nutrient depletion. Identifying the genes under SigB control that contribute to thermal tolerance will require further investigation.

A relevant observation of this study is the convergence to a common thermal resistance for the highest isothermal treatment temperature. This is aligned with previous results (Clemente-Carazo et al., 2021; Georgalis et al., 2022) and it could be due to the shorter treatment times, resulting in cells not having time to react to the treatment. Consequently, differences in the stress-response machinery at the strain level would lose relevance. This hypothesis is supported by research showing that the induction of the gene encoding SigB following heat exposure would be detected after 3 min of exposure (van der Veen et al., 2007). Therefore, it would lose relevance for situations where the microbial population is inactivated before those 3 min.

4.2. Role of the stressosome on the inactivation kinetics of L. monocytogenes

The stressosome is a multi-protein complex that functions as a sensor by integrating various stress signals, including heat stress, to initiate the signaling cascade required to activate SigB (Guerreiro et al., 2020). The *L. monocytogenes* stressosome is composed of RsbR1 (Lmo0899) and its paralogs RsbR2 (Lmo0161), RsbL (Lmo0799), RsbR3 (Lmo1642), RsbS and RsbT (Impens et al., 2017). Our results support this hypothesis, underlining the role of the stressosome in the heat resistance of *L. monocytogenes*. Comparable thermoresistance was observed between the WT strain and the RsbR1-only mutant when exposed to isothermal treatments above 55 °C. This result is reasonable based on the role of RsbR1-only in the acid stress response, where RsbR1-only can activate SigB in response to stress, even in the absence of the other four paralogs, RsbR2, RsbR3, RsbR4 and RsbL, since it still has a functional stressosome (Guerreiro et al., 2022).

Exponential phase cells of the RsbR1-only mutant showed a thermal resistance similar to the WT strain. However, this mutant had the shortest shoulder length among all strains tested in the exponential phase, but not in the stationary phase, suggesting that one of the other RsbR1 paralogues may play a role in sensing heat stress at lower temperatures (55 °C) during the exponential phase. The increased sensitivity of the Δ*sigB* mutant in both growth phases suggests that SigB regulation remains functional in the RsbR1-only strain.

The rsbR1 T241A mutant exhibited a hyperresistant phenotype, displaying a resistance higher than even the WT strain. This finding is consistent with previous studies, as exponential phase cells of rsbR1 T241A also demonstrated higher acid resistance. This was attributed to a mutation in putative phosphorylation sites in the core proteins of the stressossome RsbR1 that elevates basal SigB activity (Guerreiro et al., 2022).

The other two mutant strains studied (rsbS S56A and rsbT N49A) had lower heat resistance under isothermal conditions than the wild type

strain. This is aligned with previous studies, where these mutants also exhibited lower acid resistance compared to the wild type strain (Guerreiro et al., 2022). This is likely associated with an impeded SigB activation, as the mutations introduced in these strains disrupt signal transduction within the SigB regulatory pathway. Specifically, the mutation in the kinase RsbT loses its ability to phosphorylate RsbR1 and RsbS, regardless of stress conditions, and is consequently unable to activate SigB (Dessaux et al., 2020). The substitution of the phosphorylated serine residue with alanine in RsbS (rsbS S56A) also abolishes SigB activation (Guerreiro et al., 2022). Therefore, either mutation would disrupt SigB activation, ultimately resulting in a lower thermal resistance.

4.3. The case of microbial kinetics during dynamic heating profiles

One of the most innovative aspects of this research is the consideration of dynamic treatments, as most previous studies analysed the role of SigB for isothermal treatments only. Dynamic treatments with a long heating phase expose the cells to sublethal temperatures that might induce adaptive strategies that facilitate acclimatization. Consistently with previous studies (Clemente-Carazo et al., 2020; Garre et al., 2018; Georgalis et al., 2023; González-Tejedor et al., 2023), a longer heating phase would allow bacterial cells to develop greater acclimatization to the stress ultimately increasing their thermal resistance. This effect would practically disappear for heating rates of 14 °C/min or higher, resulting in a thermal resistance comparable to the isothermal one.

SigB might be expected to participate in this dynamic stress acclimation by regulating the stress response. However, at slower heating rates (2 °C/min), the differences between the WT and mutant strains were minimal, suggesting that the gradual temperature increase allowed cells to acclimate independently of SigB activity. This suggests that SigB plays a limited role in dynamic heat stress acclimation of *L. monocytogenes*. This is in line with previous studies observing that pre-adaptation to sublethal temperatures had a similar effect on thermal resistance for a WT and a Δ*sigB* mutant (Georgalis, Yeak, et al., 2023). Although those studies were based on *Bacillus subtilis*, it is reasonable to assume that there are similarities in the stress response of *L. monocytogenes* and *B. subtilis*, as both share a stressosome and SigB.

The acclimation of *L. monocytogenes* to heat involves not only the expression of SigB-dependent genes (Class II stress response genes), but also specific heat shock regulators (Class I and Class III heat shock genes) and SOS response (Bucur, Grigore-Gurgu, Crauwels, Riedel, & Nicolau, 2018; van der Veen et al., 2007). Class I heat-shock genes (*grpE*, *dnaK*, *dnaJ*, *groEL*, and *groES*) encode heat shock proteins (HSPs), whose principal function is to stabilize and assist protein folding (Roncarati & Scarlato, 2017). The expression of class I heat-shock genes is up-regulated for cells growing under stressful growth conditions (Bucur et al., 2018), as evidenced by chaperones of this group (GroEL and GroES) being overexpressed for exponential phase cells grown above 37 °C (Won, Lee, Kim, Choi, & Kim, 2020). Class III heat-shock genes encode for ATP-dependent proteases (ClpC, ClpP, and ClpE) that degrade damaged or misfolded proteins (Krüger, Witt, Ohlmeier, Hanschke, & Hecker, 2000) and are induced during heat shock (van der Veen et al., 2007). In turn, the negative transcriptional regulators HrcA and CtsR regulate class I and class III heat shock genes, respectively (Bucur et al., 2018; Chaturongakul et al., 2011). The stress response mechanisms of this microorganism are the result of the overexpression of genes regulated by both transcriptional regulators (Hu et al., 2007; Nair, Derré, Msadek, Gaillot, & Berche, 2000). Therefore, despite the key role of SigB, the adaptive response of *L. monocytogenes* to heat is not the result of a single system. Particularly, it is reasonable to assume that class I heat-shock genes would be up-regulated during the initial stages of the heating phase. Then, as the temperature increases, class I heat-shock genes would be downregulated while class II and III would be up-regulated.

Additional regulatory pathways and heat-stress response mechanisms in *L. monocytogenes* beyond those studied here may also contribute to cellular acclimation through distinct regulatory networks. This study clearly shows how stress acclimation can be highly significant for thermal resistance, being more impactful than, for instance, strain variability. Hence, understanding these complex interactions and incorporating them in kinetic models is crucial to improve risk predictions. Additional studies are needed to fully elucidate the adaptation process, as they could provide new insights into stress tolerance strategies, offering a biological basis for predictive models. This would ultimately enable more accurate assessment of bacterial survival under various environmental conditions, helping mitigate *L. monocytogenes* contamination in food processing environments.

4.4. Limitations and future research avenues

One limitation of our study is the lack of specific transcriptomic or proteomic analysis. Instead, our interpretation of the results is based on the analyses by Guerreiro et al. (2020). Nonetheless, it is highly unlikely that there are significant differences in gene expression between both studies. The study is based on strains with mutations targeted to specific stress response mechanisms (SigB or the stressosome). Therefore, it is reasonable to assume that gene expression in response to stress would be similar in both cases. This is further supported by a qualitative analysis of the results, which shows strong similarities (e.g., the Δ*sigB* mutant being the least resistant or the rsbR1 T241A strain showing the highest resistance).

Another limitation of this research is being limited to laboratory medium. Most food products are complex matrices that affect the thermal resistance of microorganisms both due to their microstructure and their composition (Maté et al., 2017; Verheyen et al., 2020). Nonetheless, current studies on the matrix effect are limited to the population level, so the interaction between SigB and the food matrix remains mostly unexplored. This is most likely due to the large knowledge gaps that still surround SigB, so the state-of-the-art is still limited to laboratory conditions (Domen, Porter, McIntyre, Waite-Cusic, & Kovacevic, 2025; Dou et al., 2024; Xu, Ren, Zhang, Han, & Kong, 2025; Zhou et al., 2025). This limitation presents a clear next step on this research line. Complex food matrices will most certainly affect the “baseline” heat resistance (Verheyen et al., 2020), as well as SigB expression. This should be elucidated by follow-up studies that apply similar experimental designs using a food matrix instead of laboratory media (ideally supported by transcriptomic and/or proteomic analyses).

Nevertheless, we believe that it is important to first understand and quantify the effect on simple, laboratory media. This study has taken a step towards linking SigB expression and thermal resistance, defining possible ranges of variations for the *D*-value and shoulder length. However, this has been based on the Geeraerd model, which is an empirical model that makes strong simplifications at the population level. Hence, future studies should solidify the link between gene expression and microbial kinetics, by defining novel model approaches that use as variables the expression of relevant stress response genes.

5. Conclusions

Our results emphasize the limitations of “baseline” thermal resistance when predicting the ability of *L. monocytogenes* to survive heat treatments. Bacterial cells are dynamic entities, where the activation of SigB through the stressosome plays a key role in the kinetics of *L. monocytogenes*. This is evidenced by mutated strains where SigB was absent or had impeded activation showing increased sensitivity, whereas conditions leading to increased SigB activity (transition to stationary growth phase or application of low heating rates) increased thermal resistance. The effect of these adaptive mechanisms was very relevant, affecting both the *D*-value and shoulder length (up to 5-fold increase in both parameters). Therefore, future research should aim at incorporating adaptive mechanisms, as well as genotypic

characteristics, into predictive models. Nevertheless, dynamic heat treatments induced stress acclimation even in mutants where SigB was absent or impeded, so other regulatory pathways and factors beyond SigB would also play roles in the survival of *L. monocytogenes* under stress, suggesting a complex interplay of mechanisms beyond just SigB activation. Additional studies are needed to better understand how these mechanisms interact and how they are translated into changes in the microbial survival at the population level, including their interaction with matrix effects. This would enable an improvement of current kinetic models for microbial inactivation, ultimately resulting in better risk assessments.

Supplementary data to this article can be found online at https://doi.org/10.1016/j.foodres.2025.117165.

CRediT authorship contribution statement

Silvia Guillén: Writing – review & editing, Visualization, Methodology, Investigation, Formal analysis, Conceptualization. **Pablo S. Fernández:** Writing – review & editing, Visualization, Validation, Project administration, Funding acquisition, Conceptualization. **Conor O'Byrne:** Writing – review & editing, Validation, Investigation, Formal analysis, Conceptualization. **Alberto Garre:** Writing – review & editing, Writing – original draft, Software, Investigation, Conceptualization.

Declaration of competing interest

The authors declare that they have no known competing financial interests or personal relationships that could have appeared to influence the work reported in this paper.

Acknowledgments

This Research was partly funded with project PID2023-149211OB-C31 by the Spanish Ministry of Science Innovation and Universities and the Spanish Agency for Research, as well as by the AGROALNEXT programme and was supported by MCIN with funding from European Union NextGenerationEU (PRTR-C17.I1), by Fundación Séneca with funding from Comunidad Autónoma Región de Murcia (CARM), as well as by project 22574/JLI/24 from Fundación Séneca. Alberto Garre acknowledges being funded by a Ramon y Cajal Fellowship (RYC-2021-034612-I). Silvia Guillén acknowledges the financial support of Margarita Salas Grant from University of Zaragoza, funded by the European Union "NexGenerationEU". Conor O'Byrne acknowledges support from the Science Foundation Ireland Frontiers for the Future Programme (21/FFP-P/10 078).

Data availability

Data will be made available on request.

References

van Asselt, E. D., & Zwietering, M. H. (2006). A systematic approach to determine global thermal inactivation parameters for various food pathogens. *International Journal of Food Microbiology, 107*, 73–82. https://doi.org/10.1016/j.ijfoodmicro.2005.08.014

Bates, D. M., & Watts, D. G. (2007). *Nonlinear regression analysis and its applications* (1st ed.). New York, NY: Wiley-Interscience.

den Besten, H. M. W., Aryani, D. C., Metselaar, K. I., & Zwietering, M. H. (2017). Microbial variability in growth and heat resistance of a pathogen and a spoiler: All variabilities are equal but some are more equal than others. *International Journal of Food Microbiology, 240*, 24–31. https://doi.org/10.1016/j.ijfoodmicro.2016.04.025

Bucur, F. I., Grigore-Gurgu, L., Crauwels, P., Riedel, C. U., & Nicolau, A. I. (2018). Resistance of *Listeria monocytogenes* to stress conditions encountered in food and food processing environments. *Frontiers in Microbiology, 9*. https://doi.org/10.3389/fmicb.2018.02700

Chaturongakul, S., Raengpradub, S., Palmer, M. E., Bergholz, T. M., Orsi, R. H., Hu, Y., … Boor, K. J. (2011). Transcriptomic and phenotypic analyses identify coregulated, overlapping regulons among PrfA, CtsR, HrcA, and the alternative sigma factors σB, σC, σH, and σL in *Listeria monocytogenes*. *Applied and Environmental Microbiology, 77*, 187–200. https://doi.org/10.1128/AEM.00952-10

Clemente-Carazo, M., Cebrián, G., Garre, A., & Palop, A. (2020). Variability in the heat resistance of *Listeria monocytogenes* under dynamic conditions can be more relevant than that evidenced by isothermal treatments. *Food Research International, 137*, Article 109538. https://doi.org/10.1016/j.foodres.2020.109538

Clemente-Carazo, M., Leal, J.-J., Huertas, J.-P., Garre, A., Palop, A., & Periago, P. M. (2021). The different response to an acid shock of two Salmonella strains Marks their resistance to thermal treatments. *Frontiers in Microbiology, 12*, 2616. https://doi.org/10.3389/fmicb.2021.691248

Conesa, R., Andreu, S., Fernández, P. S., Esnoz, A., & Palop, A. (2009). Nonisothermal heat resistance determinations with the thermoresistometer Mastia. *Journal of Applied Microbiology, 107*, 506–513. https://doi.org/10.1111/j.1365-2672.2009.04236.x

Dessaux, C., Guerreiro, D. N., Pucciarelli, M. G., O'Byrne, C. P., & García-del Portillo, F. (2020). Impact of osmotic stress on the phosphorylation and subcellular location of *Listeria monocytogenes* stressosome proteins. *Scientific Reports, 10*, 20837. https://doi.org/10.1038/s41598-020-77738-z

Domen, A., Porter, J., McIntyre, L., Waite-Cusic, J., & Kovacevic, J. (2025). Fluoroquinolone susceptibility of wild-type *Listeria monocytogenes* isolates and the role of FepR and ParC mutations in conferring fluoroquinolone tolerance. *International Journal of Food Microbiology, 441*, Article 111290. https://doi.org/10.1016/j.ijfoodmicro.2025.111290

Dorey, A. L., Lee, B.-H., Rotter, B., & O'Byrne, C. P. (2019). Blue light sensing in *Listeria monocytogenes* is temperature-dependent and the transcriptional response to it is predominantly SigB-dependent. *Frontiers in Microbiology, 10*, 2497. https://doi.org/10.3389/fmicb.2019.02497

Dou, X., Liu, Y., Koutsoumanis, K., Song, C., Li, Z., Zhang, H., … Dong, Q. (2024). Employing genome-wide association studies to investigate acid adaptation mechanisms in Listeria monocytogenes. *Food Research International, 196*, Article 115106. https://doi.org/10.1016/j.foodres.2024.115106

Ferreira, A., O'Byrne, C. P., & Boor, K. J. (2001). Role of σb in heat, ethanol, acid, and oxidative stress resistance and during carbon starvation in *Listeria monocytogenes*. *Applied and Environmental Microbiology, 67*, 4454–4457. https://doi.org/10.1128/AEM.67.10.4454-4457.2001

Garre, A., Egea, J. A., Iguaz, A., Palop, A., & Fernandez, P. S. (2018). Relevance of the induced stress resistance when identifying the critical microorganism for microbial risk assessment. *Frontiers in Microbiology, 9*. https://doi.org/10.3389/fmicb.2018.01663

Garre, A., Fernández, P. S., Lindqvist, R., & Egea, J. A. (2017). Bioinactivation: Software for modelling dynamic microbial inactivation. *Food Research International, 93*, 66–74. https://doi.org/10.1016/j.foodres.2017.01.012

Garre, A., Georgalis, L., Lindqvist, R., & Fernandez, P. S. (2025). Development and validation of microbial inactivation models using Bioinactivation4. In F. Pérez-Rodríguez, A. Valero, & A. Bolivar (Eds.), *Basic protocols in predictive microbiology Softwares* (pp. 13–58). US, New York, NY: Springer. https://doi.org/10.1007/978-1-0716-4112-5_2.

Garre, A., González-Tejedor, G. A., Aznar, A., Fernández, P. S., & Egea, J. A. (2019). Mathematical modelling of the stress resistance induced in *Listeria monocytogenes* during dynamic, mild heat treatments. *Food Microbiology, 84*, Article 103238. https://doi.org/10.1016/j.fm.2019.06.002

Garre, A., Valdramidis, V., & Guillén, S. (2025). Revisiting secondary model features for describing the shoulder and lag parameters of microbial inactivation and growth models. *International Journal of Food Microbiology, 431*, Article 111078. https://doi.org/10.1016/j.ijfoodmicro.2025.111078

Garre, A., Zwietering, M. H., & den Besten, H. M. W. (2023). The importance of what we cannot observe: Experimental limitations as a source of bias for meta-regression models in predictive microbiology. *International Journal of Food Microbiology, 387*, Article 110045. https://doi.org/10.1016/j.ijfoodmicro.2022.110045

Geeraerd, A. H., Herremans, C. H., & Van Impe, J. F. (2000). Structural model requirements to describe microbial inactivation during a mild heat treatment. *International Journal of Food Microbiology, 59*, 185–209. https://doi.org/10.1016/S0168-1605(00)00362-7

Georgalis, L., Fernandez, P. S., & Garre, A. (2023). A protocol for predictive modeling of microbial inactivation based on experimental data. In V. O. Alvarenga (Ed.), *Basic protocols in predictive food microbiology, methods and protocols in food science* (pp. 79–119). New York, NY: Springer US. https://doi.org/10.1007/978-1-0716-3413-4_5.

Georgalis, L., Psaroulaki, A., Aznar, A., Fernández, P. S., & Garre, A. (2022). Different model hypotheses are needed to account for qualitative variability in the response of two strains of *Salmonella* spp. under dynamic conditions. *Food Research International, 158*, Article 111477. https://doi.org/10.1016/j.foodres.2022.111477

Georgalis, L., Yeak, K. Y. C., Tsimpou, C., Fernandez, P. S., Wells-Bennik, M., & Garre, A. (2023). Disentangling the contributions of initial heterogeneities and dynamic stress adaptation to nonlinearities in bacterial survival curves. *Food Research International, 173*, Article 113385. https://doi.org/10.1016/j.foodres.2023.113385

González-Tejedor, G. A., Garre, A., Iguaz, A., Wong-Zhang, R., Fernández, P. S., & Possas, A. (2023). Dynamic thermal treatments in green coconut water induce dynamic stress adaptation of *Listeria innocua* that increases its thermal resistance. *Foods, 12*, 4015. https://doi.org/10.3390/foods12214015

Guerreiro, D. N., Arcari, T., & O'Byrne, C. P. (2020). The σB-mediated general stress response of *Listeria monocytogenes*: Life and death decision making in a pathogen. *Frontiers in Microbiology, 11*, 1505. https://doi.org/10.3389/fmicb.2020.01505

Guerreiro, D. N., Pucciarelli, M. G., Tiensuu, T., Gudynaite, D., Boyd, A., Johansson, J., … O'Byrne, C. P. (2022). Acid stress signals are integrated into the σB-dependent general stress response pathway via the stressosome in the food-borne pathogen *Listeria monocytogenes*. *PLoS Pathogens, 18*, Article e1010213. https://doi.org/10.1371/journal.ppat.1010213

Heinrich, V., Zunabovic, M., Petschnig, A., Müller, H., Lassenberger, A., Reimhult, E., & Kneifel, W. (2016). Previous homologous and heterologous stress exposure induces tolerance development to pulsed light in *Listeria monocytogenes*. *Frontiers in Microbiology, 7*. https://doi.org/10.3389/fmicb.2016.00490

Hu, Y., Raengpradub, S., Schwab, U., Loss, C., Orsi, R. H., Wiedmann, M., & Boor, K. J. (2007). Phenotypic and transcriptomic analyses demonstrate interactions between the transcriptional regulators CtsR and sigma B in *Listeria monocytogenes*. *Applied and Environmental Microbiology, 73*, 7967–7980. https://doi.org/10.1128/AEM.01085-07

Huang, L. (2009). Thermal inactivation of Listeria monocytogenes in ground beef under isothermal and dynamic temperature conditions. *Journal of Food Engineering, 90*, 380–387. https://doi.org/10.1016/j.jfoodeng.2008.07.011

Impens, F., Rolhion, N., Radoshevich, L., Bécavin, C., Duval, M., Mellin, J., … Cossart, P. (2017). N-terminomics identifies Prli42 as a membrane miniprotein conserved in Firmicutes and critical for stressosome activation in *Listeria monocytogenes*. *Nature Microbiology, 2*, 1–12. https://doi.org/10.1038/nmicrobiol.2017.5

Krüger, E., Witt, E., Ohlmeier, S., Hanschke, R., & Hecker, M. (2000). The Clp proteases of bacillus subtilis are directly involved in degradation of misfolded proteins. *Journal of Bacteriology, 182*, 3259–3265. https://doi.org/10.1128/jb.182.11.3259-3265.2000

Liu, Y., Ma, X., Cazzaniga, M., Gahan, C. G. M., den Besten, H. M. W., & Abee, T. (2025). Nano in Micro: Novel concepts in foodborne pathogen transmission and pathogenesis. *Annual Review of Food Science and Technology, 16*, 245–268. https://doi.org/10.1146/annurev-food-111523-121811

Liu, Y., Orsi, R. H., Boor, K. J., Wiedmann, M., & Guariglia-Oropeza, V. (2017). Home alone: Elimination of all but one alternative sigma factor in *Listeria monocytogenes* allows prediction of new roles for σB. *Frontiers in Microbiology, 8*. https://doi.org/10.3389/fmicb.2017.01910

Ma, X., Chen, J., Zwietering, M. H., Abee, T., & Den Besten, H. M. W. (2024). Stress resistant *rpsU* variants of *Listeria monocytogenes* can become underrepresented due to enrichment bias. *International Journal of Food Microbiology, 416*, Article 110680. https://doi.org/10.1016/j.ijfoodmicro.2024.110680

Ma, X., Tempelaars, M. H., Zwietering, M. H., Boeren, S., O'Byrne, C. P., den Besten, H. M. W., & Abee, T. (2024). A single point mutation in the *Listeria monocytogenes* ribosomal gene rpsU enables SigB activation independently of the stressosome and the anti-sigma factor antagonist RsbV. *Frontiers in Microbiology, 15*, 1304325. https://doi.org/10.3389/fmicb.2024.1304325

Marles-Wright, J., Grant, T., Delumeau, O., van Duinen, G., Firbank, S. J., Lewis, P. J., Murray, J. W., Newman, J. A., Quin, M. B., Race, P. R., Rohou, A., Tichelaar, W., van Heel, M., & Lewis, R. J. (2008). Molecular architecture of the "stressosome," a signal integration and transduction hub. *Science, 322*, 92–96. https://doi.org/10.1126/science.1159572

Maté, J., Periago, P. M., Ros-Chumillas, M., Grullón, C., Huertas, J. P., & Palop, A. (2017). Fat and fibre interfere with the dramatic effect that nanoemulsified D-limonene has on the heat resistance of Listeria monocytogenes. *Food Microbiology, 62*, 270–274.

Mazzotta, A. S., & Gombas, D. E. (2001). Heat resistance of an outbreak strain of *Listeria monocytogenes* in hot dog batter. *Journal of Food Protection, 64*, 321–324. https://doi.org/10.4315/0362-028X-64.3.321

Miller, F. A., Ramos, B., Gil, M. M., Brandão, T. R. S., Teixeira, P., & Silva, C. L. M. (2009). Influence of pH, type of acid and recovery media on the thermal inactivation of *Listeria innocua*. *International Journal of Food Microbiology, 133*, 121–128. https://doi.org/10.1016/j.ijfoodmicro.2009.05.007

Moré, J. J. (1978). The Levenberg-Marquardt algorithm: Implementation and theory. In *Numerical analysis* (pp. 105–116). Berlin, Heidelberg: Springer. https://doi.org/10.1007/BFb0067700.

Nadal, L., Mañas, P., & Cebrián, G. (2024). The sigma factor σB is required for the development of the growth phase- and temperature-dependent increases in thermoresistance and membrane rigidity in *Staphylococcus aureus*. *LWT, 210*, Article 116814. https://doi.org/10.1016/j.lwt.2024.116814

Nair, S., Derré, I., Msadek, T., Gaillot, O., & Berche, P. (2000). CtsR controls class III heat shock gene expression in the human pathogen *Listeria monocytogenes*. *Molecular Microbiology, 35*, 800–811. https://doi.org/10.1046/j.1365-2958.2000.01752.x

NicAogáin, K., & O'Byrne, C. P. (2016). The role of stress and stress adaptations in determining the fate of the bacterial pathogen *Listeria monocytogenes* in the food chain. *Frontiers in Microbiology, 7*. https://doi.org/10.3389/fmicb.2016.01865

Oliver, H. F., Orsi, R. H., Ponnala, L., Keich, U., Wang, W., Sun, Q., Cartinhour, S. W., Filiatrault, M. J., Wiedmann, M., & Boor, K. J. (2009). Deep RNA sequencing of *L. monocytogenes* reveals overlapping and extensive stationary phase and sigma B-dependent transcriptomes, including multiple highly transcribed noncoding RNAs. *BMC Genomics, 10*, 641. https://doi.org/10.1186/1471-2164-10-641

Peñalver-Soto, J. L., Garre, A., Esnoz, A., Fernández, P. S., & Egea, J. A. (2019). Guidelines for the design of (optimal) isothermal inactivation experiments. *Food Research International, 126*, Article 108714. https://doi.org/10.1016/j.foodres.2019.108714

Peng, J., Tang, J., Barrett, D. M., Sablani, S. S., Anderson, N., & Powers, J. R. (2017). Thermal pasteurization of ready-to-eat foods and vegetables: Critical factors for process design and effects on quality. *Critical Reviews in Food Science and Nutrition, 57*, 2970–2995. https://doi.org/10.1080/10408398.2015.1082126

Quereda, J. J., Morón-García, A., Palacios-Gorba, C., Dessaux, C., García-del Portillo, F., Pucciarelli, M. G., & Ortega, A. D. (2021). Pathogenicity and virulence of Listeria monocytogenes: A trip from environmental to medical microbiology. *Virulence, 12*, 2509–2545. https://doi.org/10.1080/21505594.2021.1975526

R Core Team. (2022). *R: A language and environment for statistical computing*. Vienna, Austria: R Foundation for Statistical Computing.

Roncarati, D., & Scarlato, V. (2017). Regulation of heat-shock genes in bacteria: From signal sensing to gene expression output. *FEMS Microbiology Reviews, 41*, 549–574. https://doi.org/10.1093/femsre/fux015

Ruiz, V., Alonso, R., Salvador, M., Condón, S., & Condón-Abanto, S. (2021). Impact of shoulders on the calculus of heat sterilization treatments with different bacterial spores. *Food Microbiology, 94*, Article 103663. https://doi.org/10.1016/j.fm.2020.103663

Smelt, J. P. P. M., & Brul, S. (2014). Thermal inactivation of microorganisms. *Critical Reviews in Food Science and Nutrition, 54*, 1371–1385. https://doi.org/10.1080/10408398.2011.637645

Soetaert, K., & Petzoldt, T. (2010). Inverse modelling, sensitivity and Monte Carlo analysis in R using package FME. *Journal of Statistical Software, 33*, 1–28. https://doi.org/10.18637/jss.v033.i03

Somolinos, M., Espina, L., Pagán, R., & Garcia, D. (2010). *sigB* absence decreased *Listeria monocytogenes* EGD-e heat resistance but not its pulsed electric fields resistance. *International Journal of Food Microbiology, 141*, 32–38. https://doi.org/10.1016/j.ijfoodmicro.2010.04.023

Szlachta, K., Keller, S. E., Shazer, A., & Chirtel, S. (2010). Thermal resistance of Listeria monocytogenes Scott a in ultrafiltered Milk as related to the effect of different Milk components. *Journal of Food Protection, 73*, 2110–2115. https://doi.org/10.4315/0362-028X-73.11.2110

Utratna, M., Cosgrave, E., Baustian, C., Ceredig, R. H., & O'Byrne, C. P. (2014). Effects of growth phase and temperature on σB activity within a *Listeria monocytogenes* population: Evidence for RsbV-independent activation of σB at refrigeration temperatures. *BioMed Research International, 2014*, Article 641647. https://doi.org/10.1155/2014/641647

Valdramidis, V. P., Geeraerd, A. H., Bernaerts, K., & Van Impe, J. F. (2006). Microbial dynamics versus mathematical model dynamics: The case of microbial heat resistance induction. *Innovative Food Science and Emerging Technologies, 7*, 80–87. https://doi.org/10.1016/j.ifset.2005.09.005

Valdramidis, V. P., Van Impe, J., & Geeraerd, A. (2006). *Modelling the performance of thermal processes with respect to microbial inactivation phenomena occuring in food (model) systems*. KU Leuven.

van der Veen, S., Hain, T., Wouters, J. A., Hossain, H., de Vos, W. M., Abee, T., Chakraborty, T., & Wells-Bennik, M. H. J. (2007). The heat-shock response of *Listeria monocytogenes* comprises genes involved in heat shock, cell division, cell wall synthesis, and the SOS response. *Microbiology, 153*, 3593–3607. https://doi.org/10.1099/mic.0.2007/006361-0

Verbeyst, L., Bogaerts, R., Van der Plancken, I., Hendrickx, M., & Van Loey, A. (2013). Modelling of vitamin C degradation during thermal and high-pressure treatments of red fruit. *Food and Bioprocess Technology, 6*, 1015–1023. https://doi.org/10.1007/s11947-012-0784-y

Verheyen, D., Govaert, M., Seow, T. K., Ruvina, J., Mukherjee, V., Baka, M., … Van Impe, J. F. M. (2020). The complex effect of food matrix fat content on thermal inactivation of Listeria monocytogenes: Case study in emulsion and gelled emulsion model systems. *Frontiers in Microbiology, 10*. https://doi.org/10.3389/fmicb.2019.03149

Wang, J., Law, C.-L., Mujumdar, A. S., & Xiao, H.-W. (2017). The degradation mechanism and kinetics of vitamin C in fruits and vegetables during thermal processing. In P. K. Nema, B. P. Kaur, & Mujumdareds (Eds.), *AS fundamentals & applications Part III* (pp. 227–253).

Wang, X., Devlieghere, F., Geeraerd, A., & Uyttendaele, M. (2017). Thermal inactivation and sublethal injury kinetics of Salmonella enterica and Listeria monocytogenes in broth versus agar surface. *International Journal of Food Microbiology, 243*, 70–77. https://doi.org/10.1016/j.ijfoodmicro.2016.12.008

Wang, X., Zheng, J., Luo, L., Hong, Y., Li, X., Zhu, Y., … Bai, L. (2024). Thermal inactivation kinetics of *Listeria monocytogenes* in milk under isothermal and dynamic conditions. *Food Research International, 179*, Article 114010. https://doi.org/10.1016/j.foodres.2024.114010

Won, S., Lee, J., Kim, J., Choi, H., & Kim, J. (2020). Comparative whole cell proteomics of *Listeria monocytogenes* at different growth temperatures. *Journal of Microbiology and Biotechnology, 30*, 259–270. https://doi.org/10.4014/jmb.1911.11027

Xu, J., Ren, J., Zhang, Y., Han, Z., & Kong, Q. (2025). The putative rho guanine nucleotide exchange factor GerA in *aspergillus flavus* regulates growth, development, and aflatoxin synthesis. *International Journal of Food Microbiology, 441*, Article 111302. https://doi.org/10.1016/j.ijfoodmicro.2025.111302

Zhou, W., Han, Y., Li, W., Deng, A., Li, Y., Xu, J., … Yang, Z. (2025). Prophage transduction promotes the transmission of phage resistance interfering with adsorption among Chinese foodborne *Staphylococcus aureus*. *International Journal of Food Microbiology, 440*, Article 111271. https://doi.org/10.1016/j.ijfoodmicro.2025.111271

Zwietering, M. H., Garre, A., & den Besten, H. M. W. (2021). Incorporating strain variability in the design of heat treatments: A stochastic approach and a kinetic approach. *Food Research International, 139*, Article 109973. https://doi.org/10.1016/j.foodres.2020.109973